Supplementary Information for

Supramolecular topological adhesion boosts delamination resistance in carbon fiber reinforced polymers

*Monica Milani,[a] Silvia D'Auria [a] Francesco Bertocchi,[a] Alice Boschetti,[d,e] Andrea Lapini,[a] Alberto Fina,[b] Alessandro Pedrini,[a] Roberta Pinalli,[a] Chiara Pernechele,[c] Enrico Dalcanale[a]**

[a] Department of Chemistry, Life Sciences and Environmental Sustainability and INSTM UdR Parma, University of Parma, Parco Area delle Scienze 17/A, 43124 Parma, Italy

[b] Dipartimento di Scienza Applicata e Tecnologia, Politecnico di Torino, Viale Teresa Michel 5, 15121 Alessandria, Italy

[c] Dallara S.p.A., Via Provinciale 33, 43040 -Varano Melegari (PR), Italy

[d]Istituto Nazionale di Ricerca Metrologica (INRIM) 10135 Torino, Italy

[e]European Laboratory for Non-Linear Spectroscopy (LENS), Sesto Fiorentino, Italy

E-mail corresponding author: enrico.dalcanale@unipr.it

Summary

Methods 2

Synthesis 4

^{1}H NMR spectra 8

ATR FT-IR spectra 9

DSC analysis 10

Viscoelastic properties 11

Single Lap Shear (SLS) tests 12

Delamination tests 15

Double Cantilever Beam (DCB) and End Notched Fracture (ENF) results 19

UV-Vis analysis 24

SEM micrographs of DCB and ENF specimens 26

Methods

General.

Nuclear magnetic resonance (NMR). NMR spectra were recorded on a Bruker Advance 400 (400 MHz). Chemical shifts are reported in parts per million (ppm). ^{1}H-NMR chemical shifts are given in reference to the residual solvent peak (2.50 ppm for deuterated dimethyl sulfoxide (DMSO-d_6).

Infrared spectroscopy (IR). Infrared absorption spectroscopy analyses were performed with a Perkin Elmer FT-IR Spectrum Two instrument in the mode of Attenuated Total Reflectance (ATR) using powder samples. The background was subtracted from every spectrum recorded.

Elemental Analysis (EA). Elemental analyses were recorded on a CHNS Thermo Fisher FlashSmart. The nitrogen content was determined by means of thermal conductivity (TC) and volumetric analysis.

Differential scanning calorimetry (DSC): Test were carried out on a TA Instruments Q20 differential scanning calorimeter, using samples of ca. 7 mg into sealed aluminum pans, under nitrogen flow. The heating rate was 10°C/min between 25 °C and 200 °C, followed by cooling (10°C/min) and second heating with the same conditions. Glass transition temperature was determined as the midpoint of the transition on the second heating. *Thermogravimetric analysis (TGA):*Test were carried out on a TA Instruments TGA Discovery (Q5000) using about 10 mg samples, heated at 10°C/min between 50 °C and 800 °C, under air or nitrogen flow.

Compression molding. Before analysis, the received materials were dried in oven at 100°C under vacuum for at least an entire night prior to being molded for the analysis that required it. All samples were molded between Teflon plates with an appropriate spacer. They were preheated for 3 minutes and hot pressed under 1 ton for another 3 minutes at 200°C for PKHB-ODIN and 150°C for PKHB-PU from compression-molded plates (Carver C12, laboratory press) unless otherwise specified.

Dynamic mechanical analysis (DMTA). DMTA analyses were carried out on bars (7 x 1 mm^2 nominal cross-section, 30 mm length) cut from compression-molded plates, tested in tensile mode on a TA Instruments Q800. Tests were done on heating ramp (2°C/min) between room temperature and 170°C, at and 1 Hz frequency in strain-controlled mode, deformation amplitude at 0.05% and 0.01 N preload. The minimum load allowed (additional end-of test criterion) was set at 0.2 MPa, to prevent possible dripping. All samples were conditioned at 23°C and 50% of relative humidity for at least 48 h before analyses. Main relaxation temperature (T_α), associated with the transition between glassy state and rubbery state, was taken at the maximum of tanδ plot.

Double Cantilever Beam (DCB) tests and End Notched Fracture (ENF) tests. DCB and ENF tests were performed with an electromechanical testing machine MTS Insight 150 kN, with 250 kN hydraulic grips. The position of the transducer LVDT is 300 mm, with a resolution of 0.001 mm. The

tensile tester is equipped with a load cell of 150 kN, with a resolution of 0.002 kN class 0.5. A ZEISS ARAMIS 3D Camera was used to monitor the crack propagation.

UV-Vis absorption. UV-Vis absorption measurements were performed with two different experimental setups. The PerkinElmer Lambda650 double beam spectrophotometer was used to measure absorption spectra of PKHB-ODIN-13% sample and to measure the absorption spectra of ODIN in DMSO and $CHCl_3$ solution. Absorbance measurements of PKHB-ODIN-13% dispersed (15% w/w) in epoxy-resin were performed using a customized spectrophotometric setup to precisely assess the spatial homogeneity of solid thin films. A wide-spectrum fiber lamp that combines deuterium and halogen light sources (DH-2000-BAL, Ocean Insight) was used to illuminate the samples. The light from the fiber output was collected using a 20x microscope objective and focused to produce a beam diameter below 2 mm on the sample surface. The transmitted light was collected with a second 20x microscope objective and directed to the fiber input of an in-fiber spectrometer (Ocean Optics USB4000). The sample was mounted on an XY motorized linear translational stage with a spatial resolution below 100 µm to enable precise sampling of homogeneity. Each spectrum is the result of an average of 100 spectra collected from respectively the white lamp, the light transmitted by the sample, and the dark signal. The absorbance of the sample was then calculated using the following expression:

$$A = -log\frac{(I_t - I_b)}{(I_o - I_b)}$$

where I_t is the light transmitted through the sample, I_b is the background (dark) signal and I_o the incident intensity.

To account for the absorption contribution of the polymeric matrix, the absorbance of the bare resin was measured then subtracted from the sample after correcting for thickness variations.

SEM micrographs. SEM micrographs were acquired on a Thermo Scientific Phenom XL instrument equipped with Back Scattering Detector (BSD). The experimental settings are indicated in each figure.

Synthesis

Unless otherwise specified, chemicals and solvents were purchased from Sigma-Aldrich and used as received. All solvents employed were laboratory grade and used as received.

Synthesis of *1-(6-Isocyanatohexyl)-3-(7-oxo-7,8-dihydro-1,8-naphthyridin-2-yl)urea* ODIN isocyanate

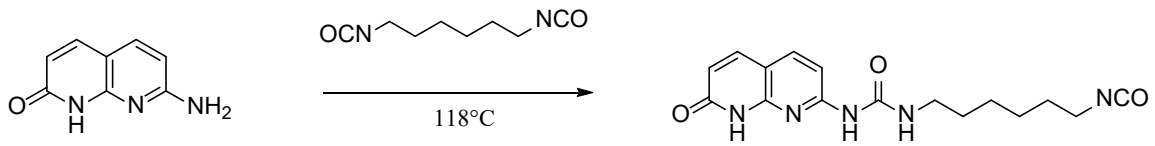

ODIN-isocyanate

Scheme S1: preparation of ODIN-isocyanate

Naphthyridine (50 g, 0.31 mol, 1 equiv) and hexamethylene diisocyanate (500 mL, 3.1 mol, 10 eq.) were combined and stirred. The resulting slurry was heated for 15 h at a temperature of 118 °C (temperature of oil bath). After cooling to room temperature, the solid was filtered over a Buchner funnel and washed with hexane and acetone until the wash was colorless. The solid residue was dried under vacuum at 60 °C, yielding the product as a tan powder with minor impurities (72.7 g, 71% yield).

^{1}H NMR (400 MHz, DMSO-d_6) δ: 12.18 (s, 1H, Ar–N*H*), 9.65 (s, 1H, Ar–N*H*–CO–NH), 8.99 (s, 1H, N*H*–CO–NH–Ar), 7.91 (d, *J* = 8.4 Hz, 1H), 7.78 (d, *J* = 9.4 Hz, 1H), 6.84 (d, *J* = 8.5 Hz, 1H), 6.34 (d, *J* = 9.4, 1.8 Hz, 1H), 3.39–3.31 (m, 2H), 3.20 (dd, *J* = 6.7 Hz, 2H), 1.62–1.48 (m, 4H), 1.43–1.19 (m, 4H). MS (ESI) *m*/*z*: $[MH]^+$ calc for $C_{17}H_{23}N_5O_4$ (ODIN isocyanate reacted with methanol), 362.18; found, 362.26.

IR, ῡ (cm-1): 3390 (N-H stretching), 2926 (C-H stretching), 2938 (C-H stretching), 2262 (N=C=O stretching), 1660 (C=O stretching, urea e lactam), 1594 (N-H bending, urea), 1533 (C-N stretching), 1242 (C-O stretching).

Synthesis of *isopropyl (6-(3-(7-oxo-7,8-dihydro-1,8-naphthyridin-2-yl)ureido)hexyl)carbamate (1)*

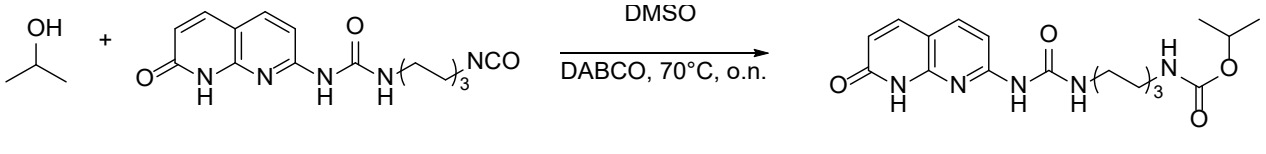

1

Scheme S2: reaction between isopropanol and ODIN-isocyanate to give model compound **1**

1-(6-isocyanatohexyl)-3-(7-oxo-7,8-dihydro-1,8-naphthyridin-2-yl)urea (100 mg, 0.23 eq.) was dissolved in 1 mL of dry DMSO, then 2-propanol (10 mL, 100 eq.) and DABCO (2 mg, 18 µmol) were added to the reaction mixture. The mixture was stirred at 70°C for one night. The product was precipitated in water and washed with water.

^{1}H NMR (600 MHz, DMSO-d_6): δ 12.13 (s, 1H, Ar−N*H*), 9.61 (s, 1H, Ar−NH−CO−N*H*), 8.94 (t, 5.9 Hz, 1H, NH−CO−N*H*), 7.87 (d, *J* = 8.6 Hz, 1H), 7.73 (d, *J* = 9,5 Hz, 1H), 6.91 (t, *J*=8.5 Hz, 1H), 6.81 (d, *J* = 5.9 Hz, 1H, N*H*−CO), 6.30 (d, *J* = 5,9 Hz, 1H), 4.68 (q, *J* = 6,18 Hz, 1H), 3.16 (d, *J* = 6.4 Hz, 2H), 2.90 (d, *J* = 6.4 Hz, 2H), 1.58 – 1.13 (m, 8H), 1.10 (d, *J* = 6.2 Hz, 4H).

IR ῡ(cm-1): 3312 (N-H stretching), 3225 (N-H stretching), 2926 (C-H stretching), 2853 (C-H stretching), 1657 (C=O stretching), 1609 (N-H bending, urea), 1513 (C-N stretching).

Synthesis of *1-(6-isocyanatohexyl)-3-phenylurea (2)*

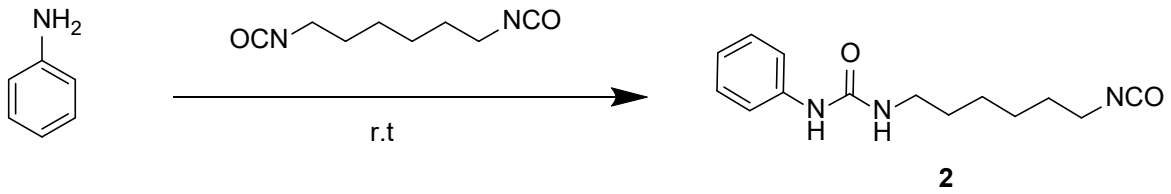

Scheme S3: preparation of PU-isocyanate

In a dry two-neck flask, aniline (1 g, 0.011 mol) and hexamethylene diisocyanate (HDI, 20 mL, 0.12 mol) were added and the reaction mixture was maintained at room temperature under stirring for four hours. Then, cyclohexane was added to promote product precipitation. The precipitate was filtered and washed with cyclohexane to remove excess HDI; the obtained white solid was dried in a vacuum oven at 40 °C for two hours (yield 91%).

^{1} H NMR (600 MHz, DMSO-d_6) δ (ppm): 8.39 (s, 1H, N*H*-C=O-NH), 7.36 (d, *J* = 7.6 Hz, 2H, CH_{Ar}), 7.22 – 7.17 (m, 2H, CH_{Ar}), 6.87 (t, , *J* = 7.3 Hz, 1H), 6.09 (t, J = 5.6 Hz, 1H, NH-C=O-N*H*), 3.35(m, 2H, CH_2-NCO), 3.06 (td, J = 6.9, 5.7 Hz, 2H, C=O-NH-CH_2), 1.56 (p, *J* = 6.7 Hz, 2H, CH_2-CH_2-NCO), 1.43 (p, *J* = 7.0 Hz, 2H, NH-CH_2-CH_2), 1.36 – 1.26 (m, 4H).

IR, ῡ(cm-1): 3319 (N-H stretching), 2933 (C-H stretching), 2958 (C-H stretching), 2262 (N=C=O stretching), 1648 (C=O stretching), 1596 (N-H bending, urea), 1551 (C-N stretching).

General procedure for the synthesis of PKHB-ODIN 8 and 13%

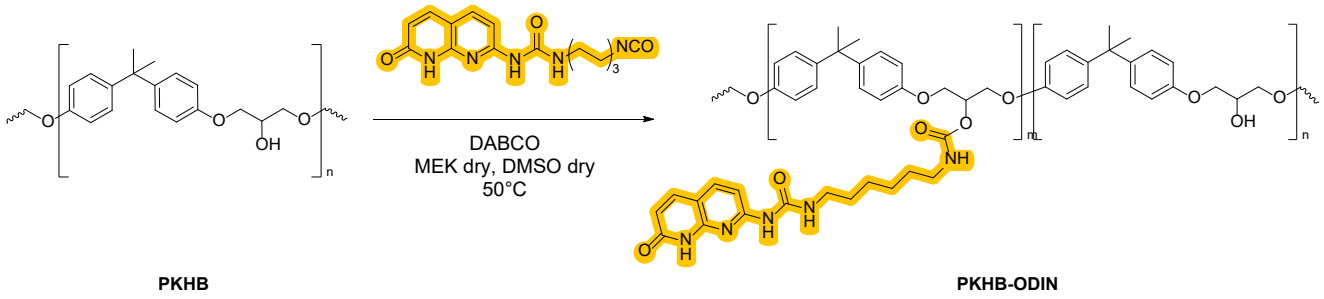

Scheme S4: preparation of PKHB-ODIN

5g of PKHB (18.0 mmol) were dissolved in 50mL of methyl ethyl ketone (MEK) at 50 °C, then DABCO (20 mg, 180 µmol) were added to the reaction mixture. Then 1.19 g (8%) or 2.38 g (13%) of 1-(6-isocyanatohexyl)-3-(7-oxo-7,8-dihydro-1,8-naphthyridin-2-yl)urea (corresponding to 3,61 mmol, 7.22 mmol ,10.8 mmol respectively) dissolved in 10, 20 mL respectively of DMSO were added under magnetic stirring. After 24 hrs in refluxing MEK, 300 mL of water are added to the solution. The resulting yellow precipitate was filtered, washed with water several times and dried in vacuum oven at 10^{-2} Torr and 60 °C for 24 h and then characterized via ^{1}H NMR (Fig. S3).

^{1}H NMR PKHB-ODIN (600 MHz, DMSO-d_6) δ ppm: 12.13 (s, Ar–N*H*), 9.62 (s, C=O-N*H*-C=N), 8.95 (s, N*H*-CO-NH-Ar), 7.91 (d, J = 8.5 Hz, C$H_{\text{Ar-ODIN}}$), 7.78 (d, J = 9.6 Hz, C$H_{\text{Ar-ODIN}}$), 7.34 (m, O-C=O-N*H*), 7.07 (d, J = 8.2 Hz, $CH_{Ar,PKHB}$,), 6.82 (d, J = 8.2 Hz, $CH_{Ar,PKHB}$), 6.64 (d, J = 8.5 Hz, C$H_{\text{Ar-ODIN}}$), 6.34 (d, J = 9.6 Hz, C$H_{\text{Ar-ODIN}}$), 5.34 (d, J = 5.3 Hz, O*H*), 5.19 (m, CH_2-C$H_{\text{PKHB-ODIN}}$-CH_2), 4.19-4.06 (m, CH_2-$CH_{PKHB-ODIN}$-CH_2, CH2-CH_{PKHB}-CH_2), 4.05-3.87 (m, CH_2-CH_{PKHB}-CH_2), 3.20 (m, C=O-NH-CH_2), 2.96 (m, CH_2-NH-C=O-O), 1.54 (s, CH_3), 1.42 – 1.16 (m, NH-CH_2-(CH_2)$_4$-CH_2-NH).

IR, ῡ (cm^{-1}): 3300 (O-H stretching), 2929 (C-H stretching), 1710 (NH(C=O)O stretching), 1233 (CO stretching, ether), 1034 (C-O stretching).

EA PKHB-ODIN 8%: Theoretical C 75.99%, H 7.28%, N 1.59%; Found C 74.68%, H 7.01%, N 1.69%.

EA PKHB-ODIN 13%: Theoretical C 74.01%, H 6.94%, N 2.42%; Found C 72.52%, H 7.02%, N 2.39%.

General procedure for the synthesis of PKHB-PU 23%

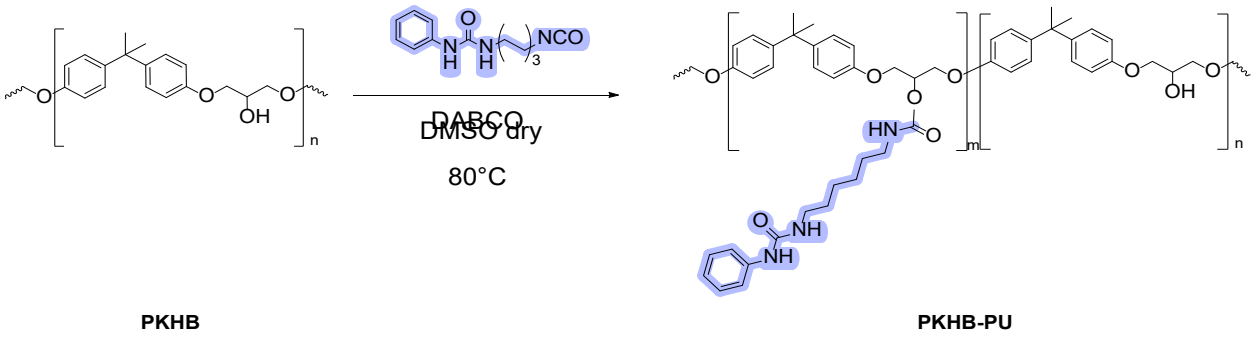

PKHB PKHB-PU

Scheme S5: preparation of PKHB-PU

5 g of PKHB (18.0 mmol) were dissolved in 50 mL of dry DMSO at 80 °C, then DABCO (20 mg, 180 µmol) is added to the reaction mixture. Then phenyl urea isocyanate (1.88 g, 7.21 mmol) is added to the reaction mixture under magnetic stirring. After 24 hrs at 80 °C the polymer is precipitated by adding 300 mL of water are added to the solution. The resulting white precipitate was filtered and dried in vacuum oven at 10^{-2} Torr and 60 °C for 24 h and then characterized via ^{1}H NMR (400 MHz, DMSO-d_6).

^{1}H NMR (400 MHz, DMSO-d_6) δ (ppm): 8.38 (s, Ar-N*H*-*C*=*O*), 7.32 (d, J = 7.7 Hz, CH-$_{\text{Ar-PU}}$-H_{orto}), 7,29 (t, J=3,52 Hz, C=O-N*H*) 7,14 (m, CH$_{\text{Ar-PU}}$-H_{meta}), 7.02 (d, J = 7.8 Hz, C$H_{Ar,PKHB}$), 6.93 (d, J=8.4 Hz, CH$_{\text{Ar-PU}}$-H_{para}), 6.81 (d, J = 7.8 Hz, C$H_{Ar,PKHB}$), 6.05 (bs, N-*H*-C=O-O), 5.34 (d, J=5.3 Hz, O*H*), 5.14 (m, CH$_2$-C*H*$_{\text{PKHB-PU}}$-CH$_2$), 4.10 (m, CH_2-C$H_{PKHB-PU}$-CH_2), 4.05 (m, CH$_2$-C*H*$_{\text{PKHB}}$-CH$_2$) 4.00 – 3.87 (m, CH_2-CH-C$H_{2\ PKHB}$), 2.99 (m, C=O-NH- CH_2), 2.92 (m, CH_2-NH-C=O-O), 1.50 (s, CH_3), 1,47-1.16 (m, NH-CH$_2$-(CH_2)$_4$-CH$_2$-NH).

IR, ῡ (cm^{-1}): 3300 (O-H stretching), 2965 (C-H stretching), 1710 (NH(C=O)O stretching), 1237 (C=O stretching, ether), 1040 (C-O stretching).

EA PKHB-PU 23%: Theoretical C, 73.97%; H, 7.15%; N, 2.80%; Found C, 72.36%, H 7.28%, N 2.96%.

Table S1: Theoretical and experimental C, H, N, S elemental analyses of the polymers synthetized. The S elemental analysis was done to exclude the presence of residual DMSO in the final products.

Elemental analyses	**%C**	**%H**	**%N**	**%S**
PKHB-ODIN 8% Theoretical	75.99%,	7.28%	1.59%	0%
PKHB-ODIN 8% Found	74.68%,	7.01%	1.69%;	0%
PKHB-ODIN 13% Theoretical	74.01%	6.94%	2.42%;	0%
PKHB-ODIN 13% Found	72.52%	7.02%	2.39%	0%
PKHB-PU 23% Theoretical	73.97%	7.15%	2.80%	0%
PKHB-PU 23% Found	72.36%	7.28%	2.96%	0%

^{1}H NMR spectra

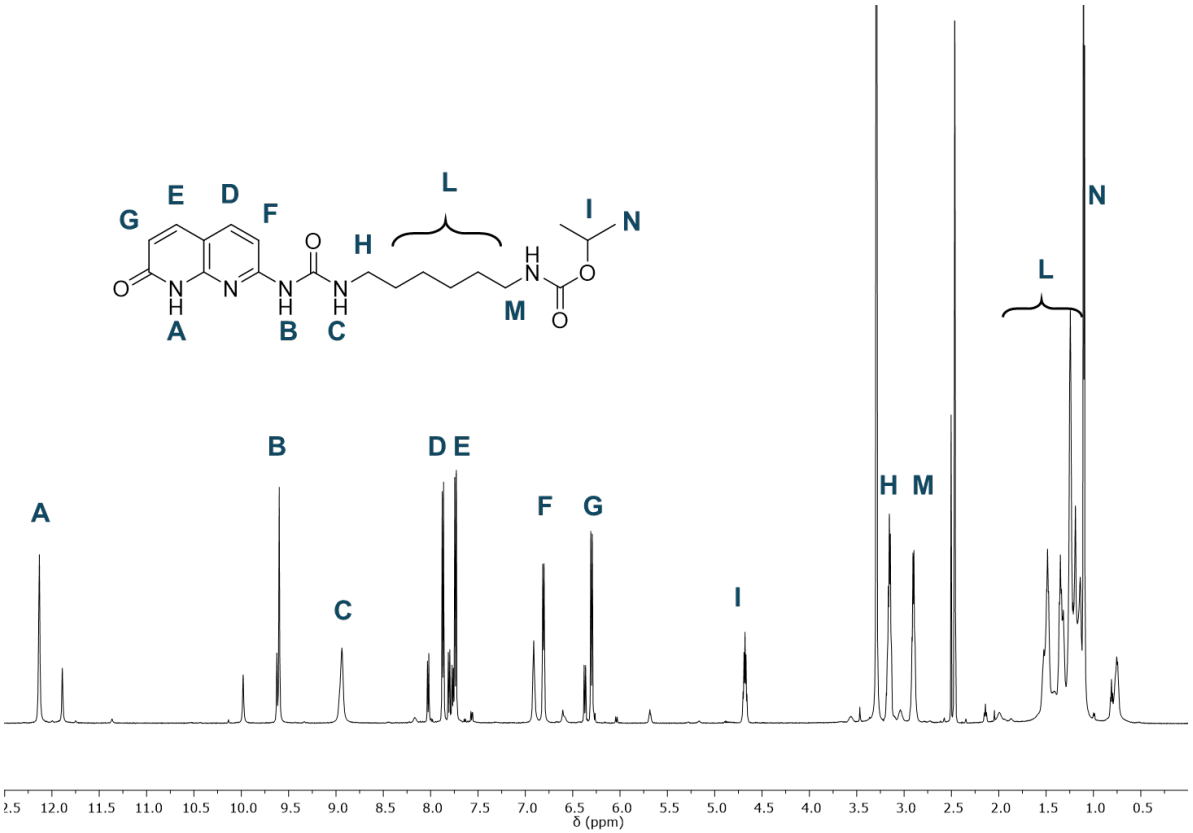

Figure S1. ^{1}H NMR (DMSO-d_6, 298K, 600 MHz): of **(1)**.

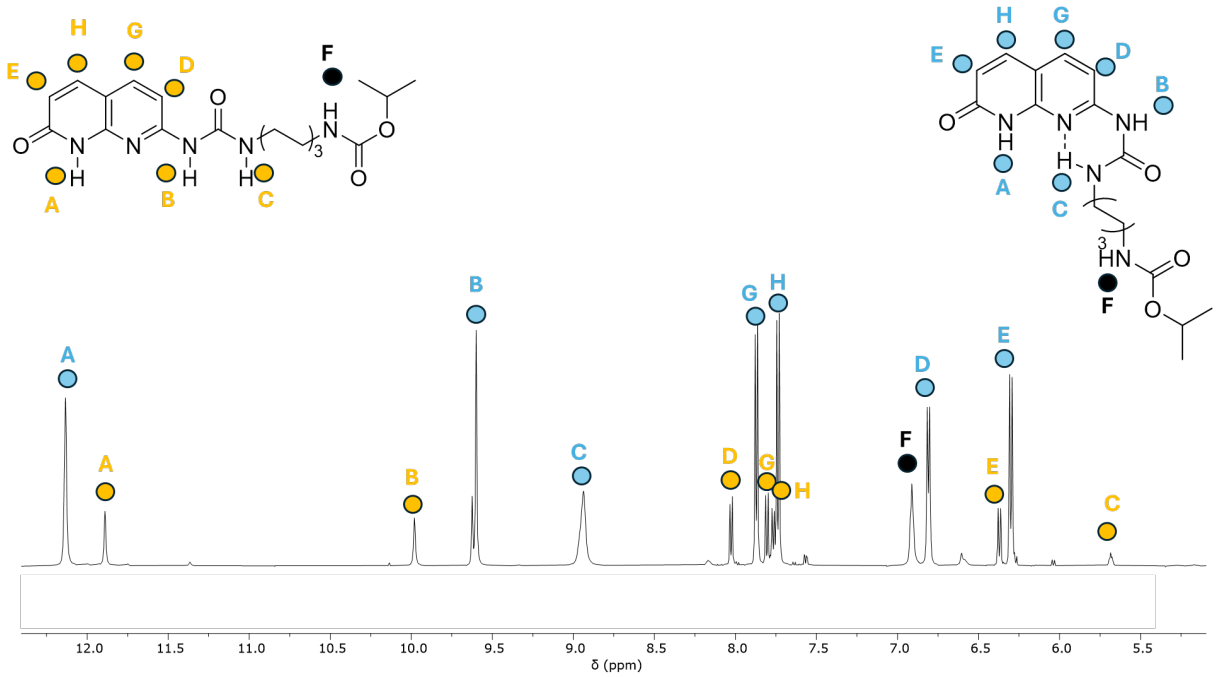

Figure S2. Expansion of the ^{1}H NMR spectrum of model compound **1** in DMSO-d_6, with the resonances assigned to the two keto tautomers: 1a (blue dots) and 1b (orange dots). Ratio **1a/1b** = 4:1

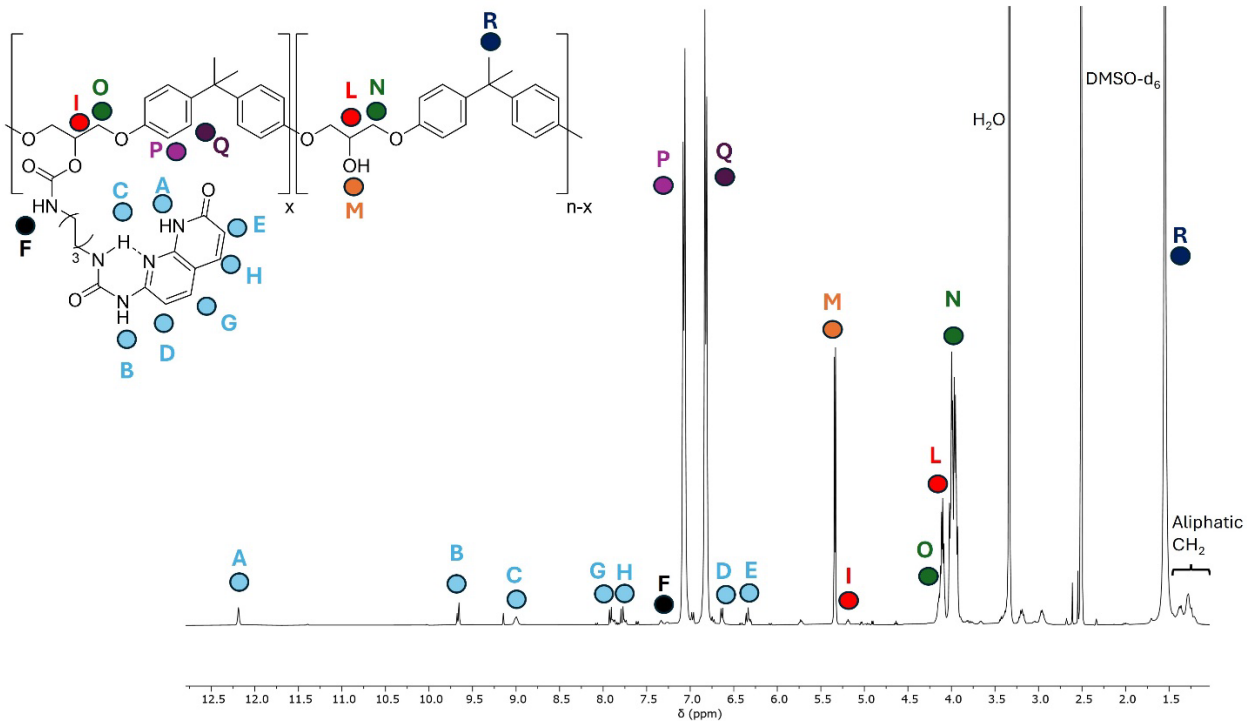

Figure S3. ^{1}H NMR (DMSO-d_6, 298K, 600 MHz): of PKHB-ODIN 8%.

ATR FT-IR spectra

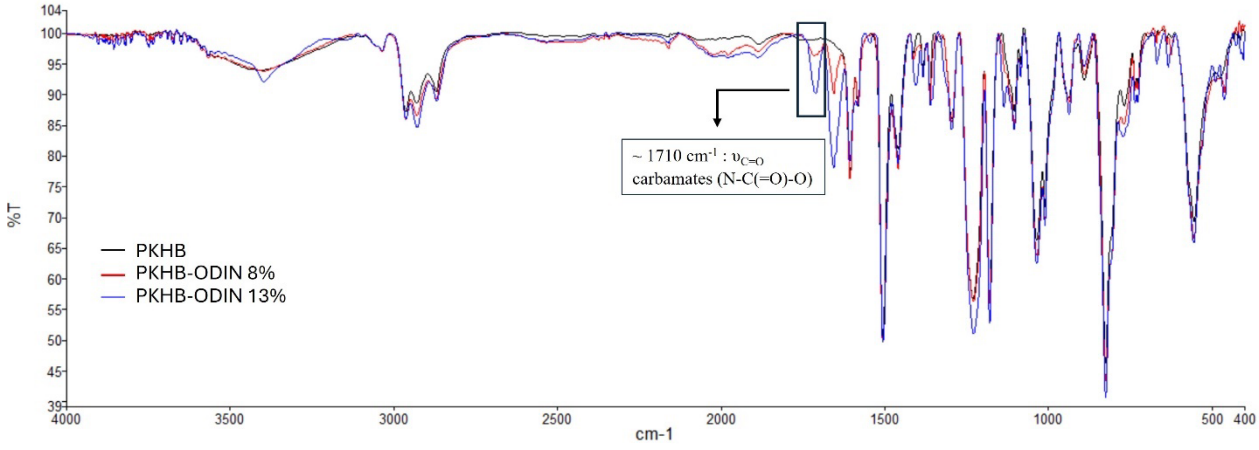

Figure S4. Comparison of ATR FT-IR spectra of PKHB (black line), PKHB-ODIN 8% (red line), PKHB-ODIN 13% (blue line).

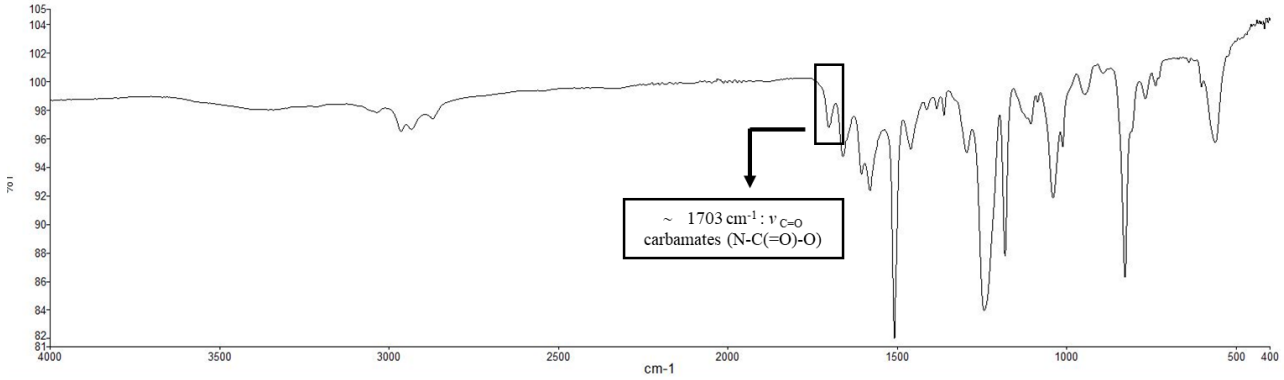

Figure S5. ATR FT-IR spectra of PKHB-PU 23%.

DSC analysis

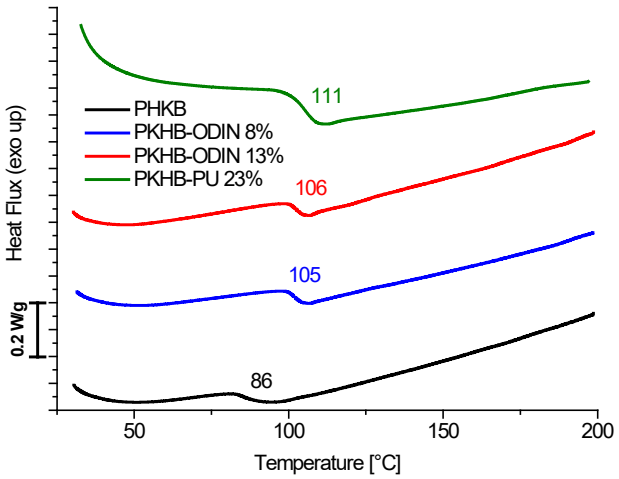

Figure S6. DSC curves of PKHB (black trace), PKHB-PU 23% (green trace) PKHB-ODIN 8% (blue trace) and PKHB-ODIN 13% (red trace).

Viscoelastic properties

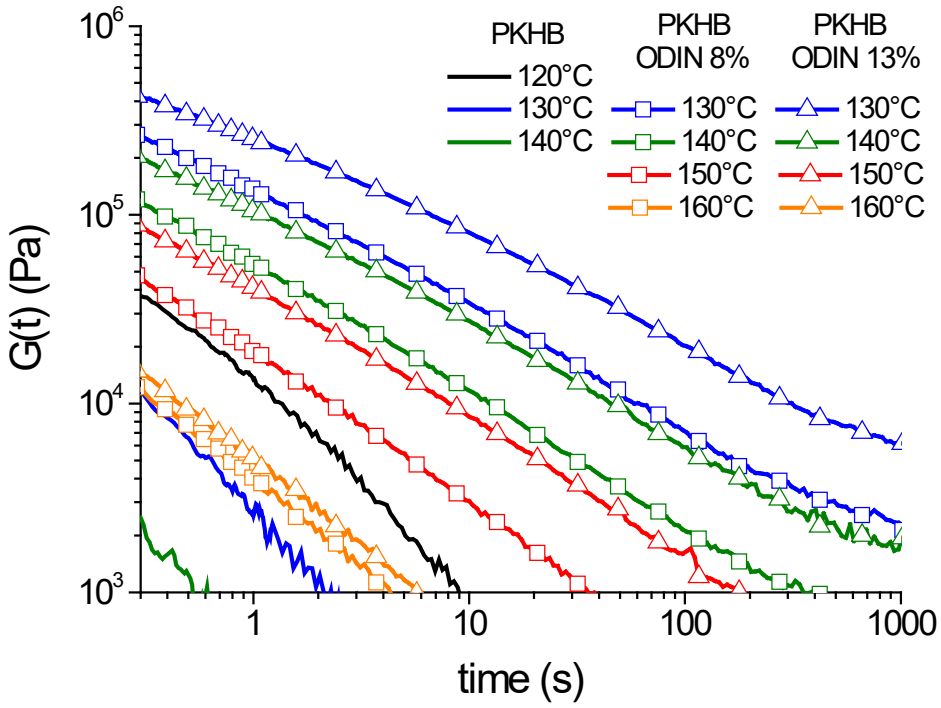

Figure S7. Stress relaxation of PKHB-ODIN 8% and PKHB-ODIN 13% vs pristine PKHB.

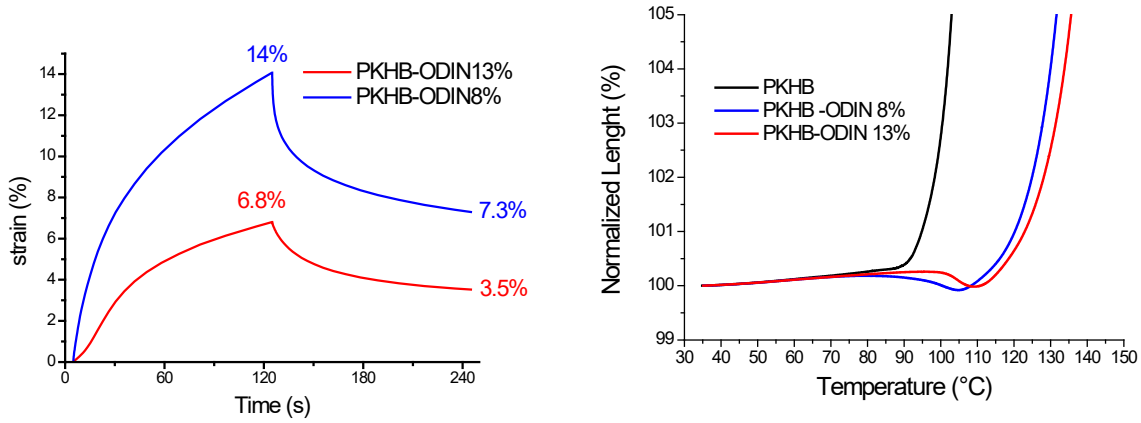

Figure S8. Isothermal creep for PKHB-ODIN 8% and PKHB-ODIN 13% at 100 °C under 100 KPa static load (a, left) and non-isothermal creep (b, right).

Single Lap Shear (SLS) tests

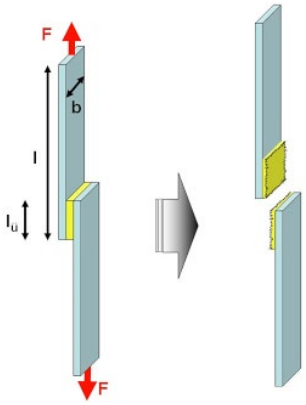

$$\tau = \frac{F}{A} = \frac{N}{mm^2} = MPa$$

Where $A = b \cdot l_u$

Figure S9. Single Lap Shear test configuration and shear strength definition.

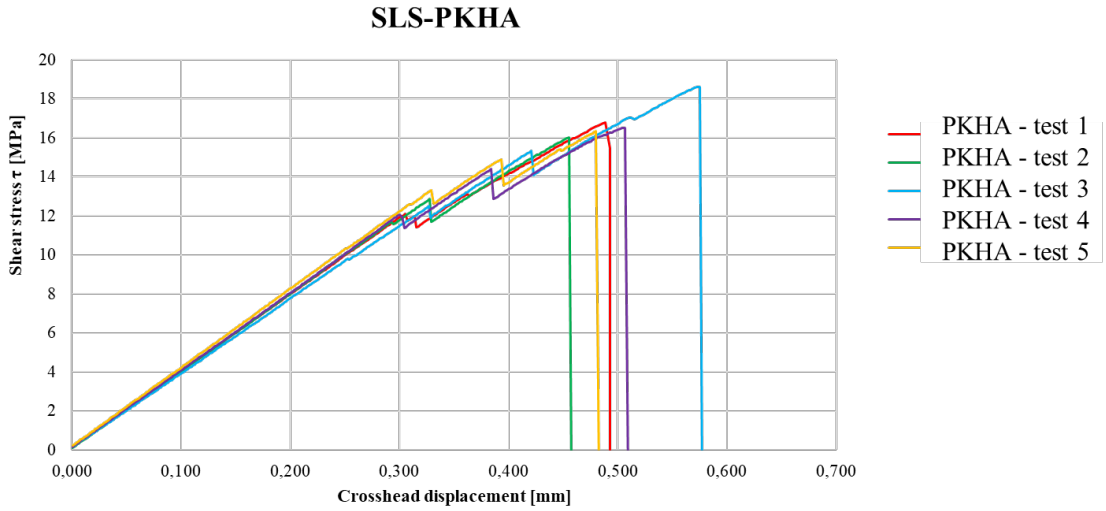

FigureS10. Stress and strain curves for specimens jointed with PKHA.

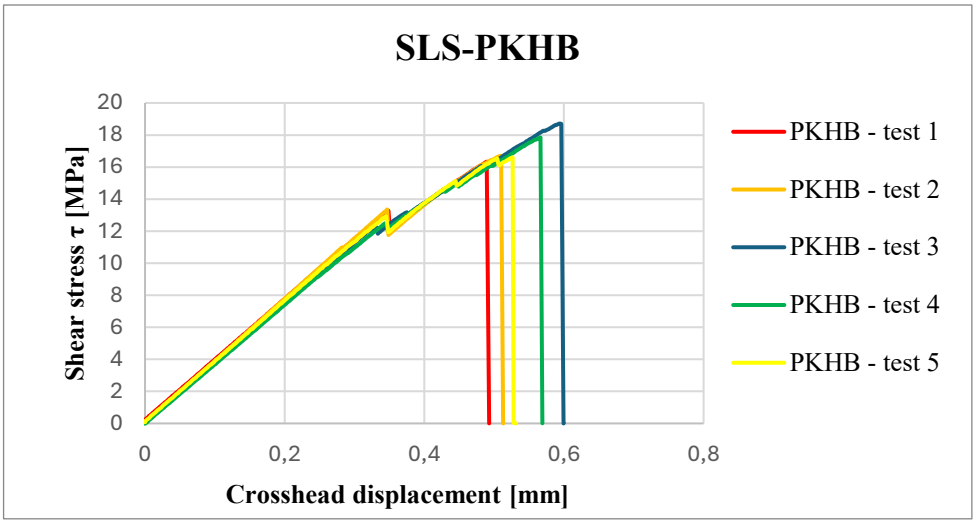

Figure S11. Stress and strain curves for specimens jointed with PKHB.

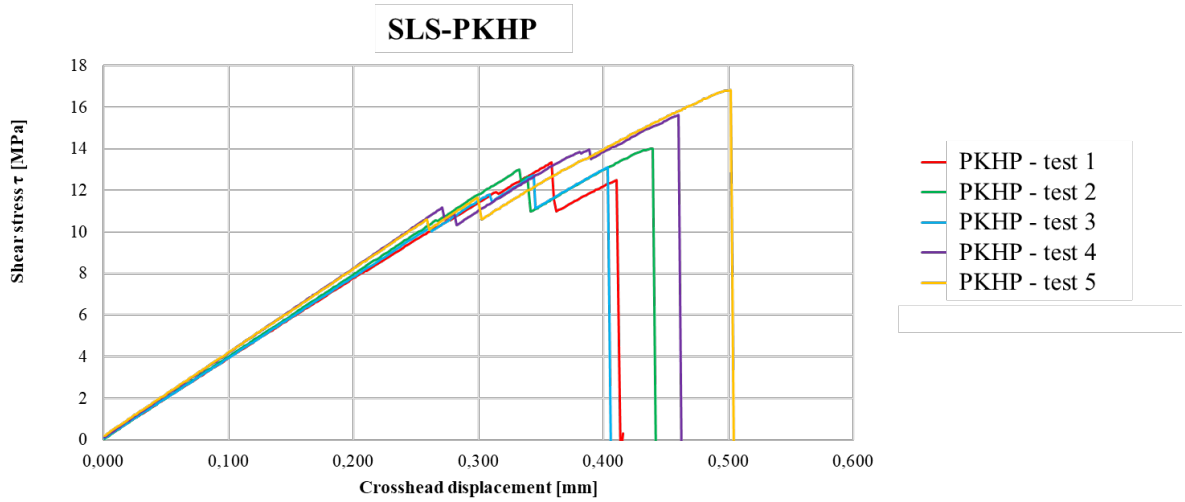

Figure S12. Stress and strain curves for specimens jointed with PKHP

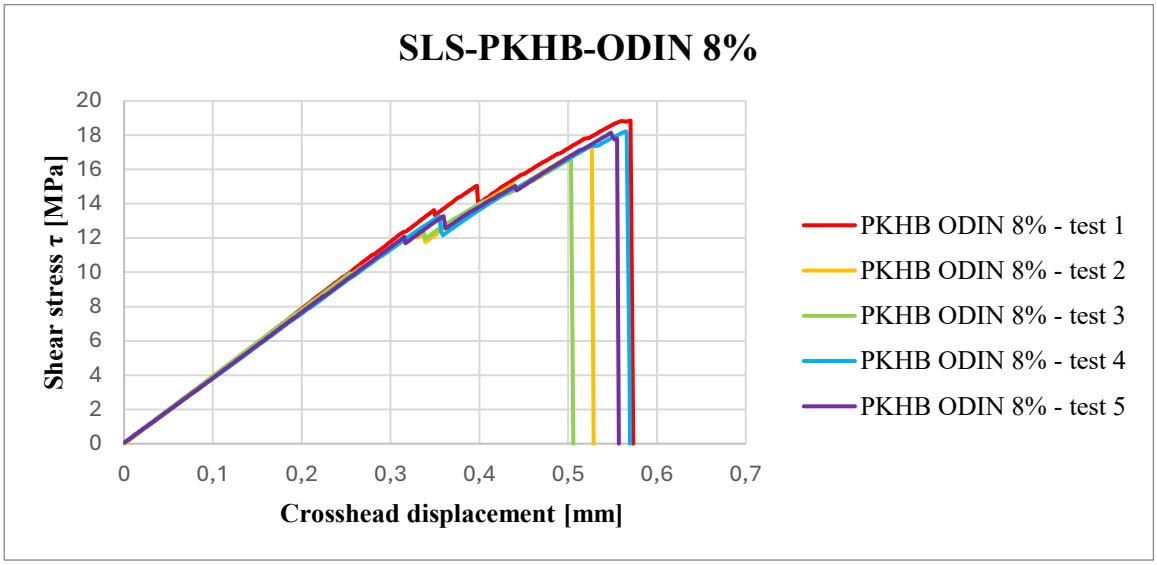

Figure S13. Stress and strain curve for specimens jointed with PKHB-ODIN 8%.

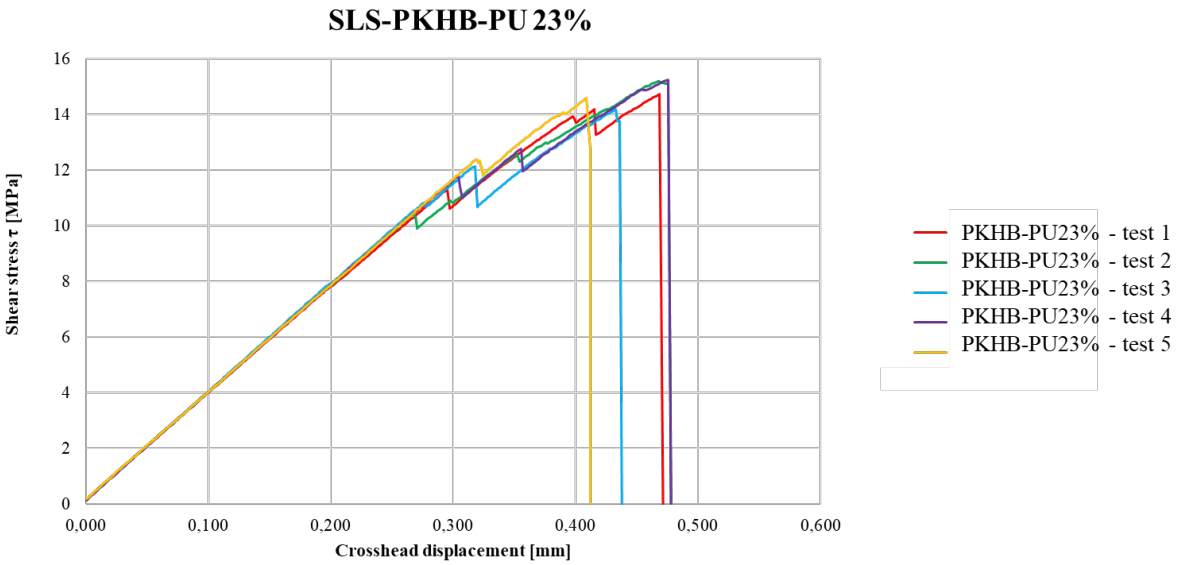

FigureS14. Stress and strain curves for specimens jointed with PKHB-PU 23%.

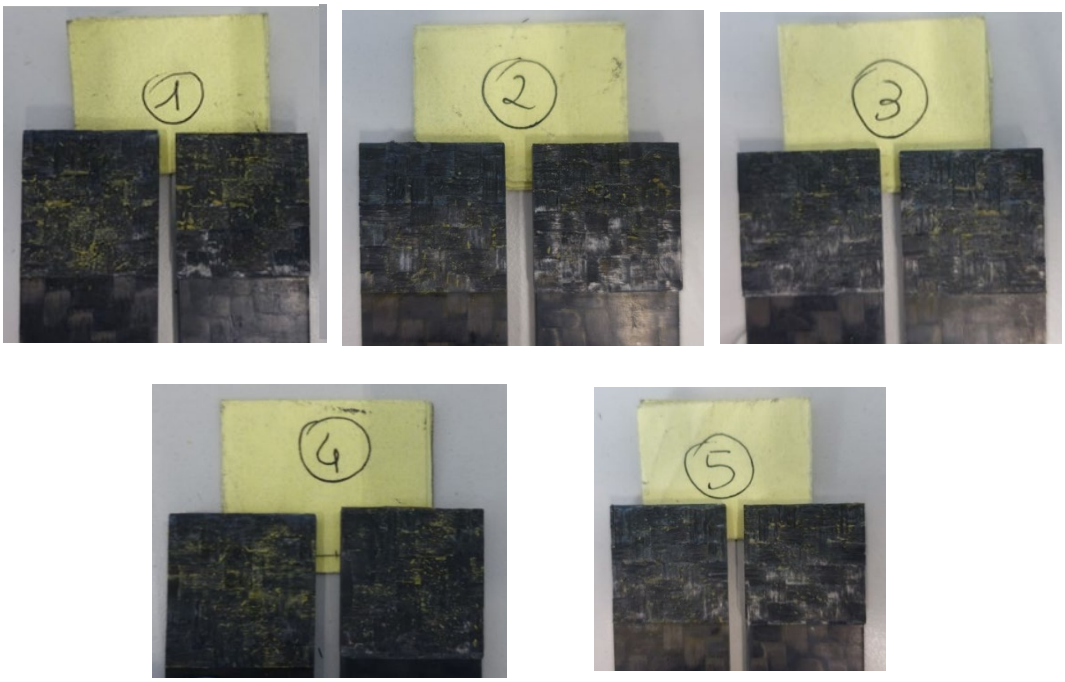

Figure S15. Photographs of cohesive rupture of SLS specimens of PKHB-ODIN 13%

Delamination tests

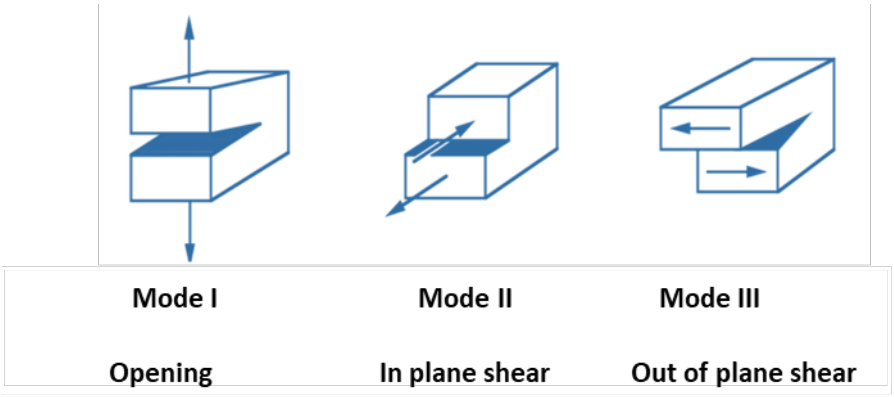

Figure S16. Delamination modes in CFRP composites.

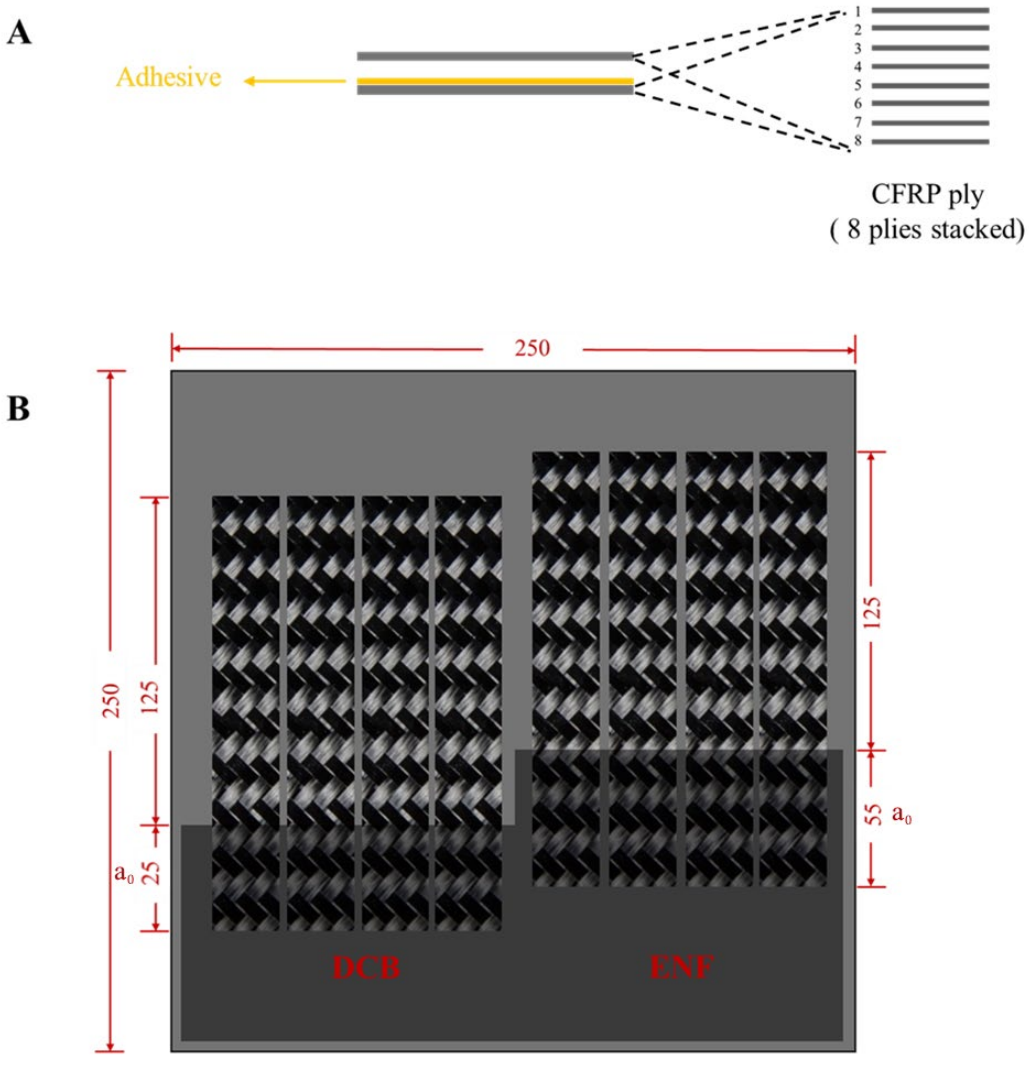

Figure S17: Stacking sequence of plies/mats for DCB and ENF panels production: (A) Reference laminates and modified laminates with the adhesives applied to the last interface of one ply. (B) Dimensions (in mm) of CFRP panels and specimens for DCB and ENF tests. The dark grey area indicates where the release of film 0.15 mm thick is applied.

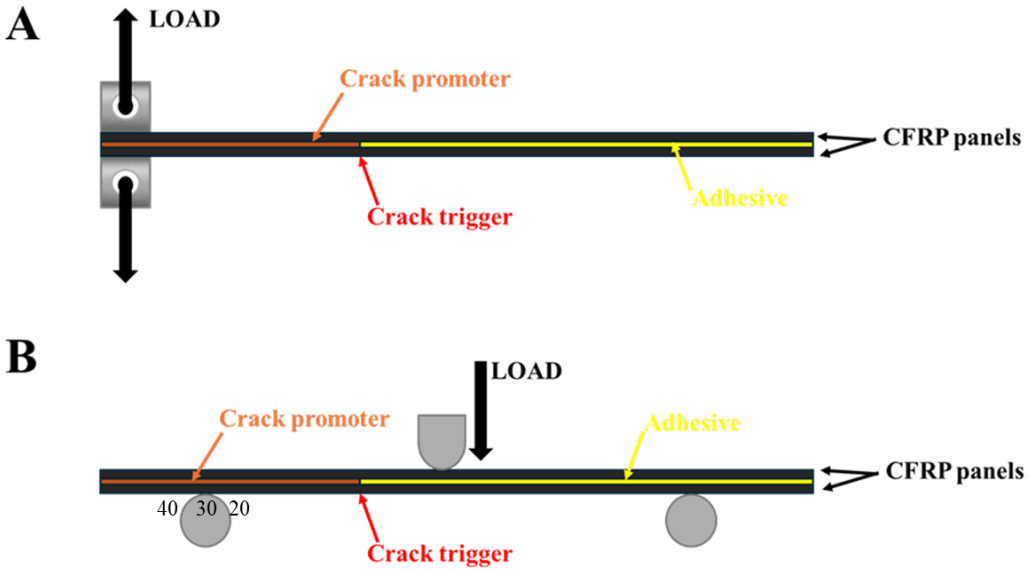

Figure S18. Schematic representation of specimens for the interlaminar fracture toughness evaluation in DCB A) and ENF (B).

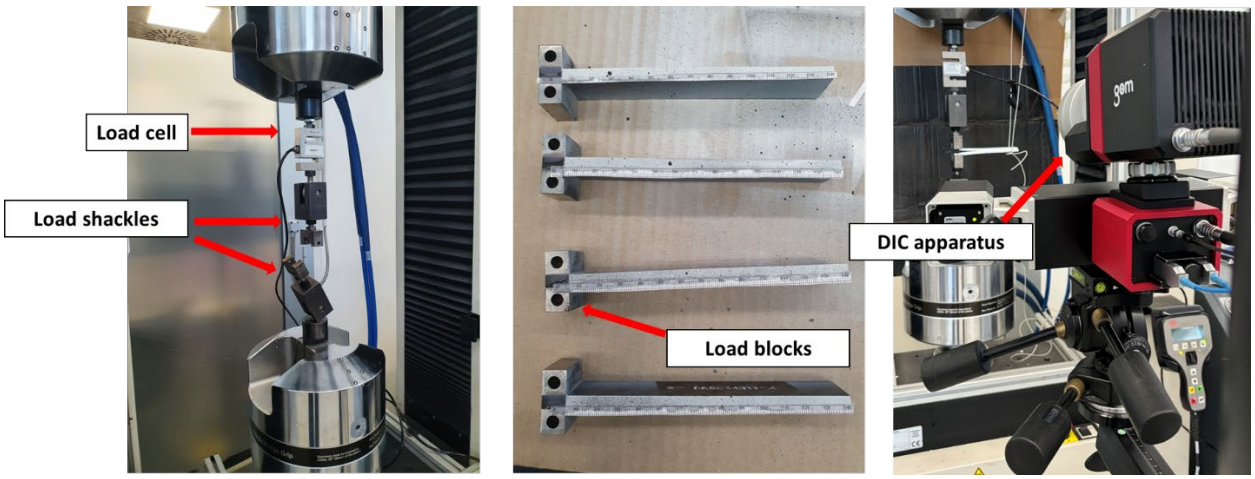

Figure S19. experimental set-up of DCB tests, its specimen and DIC camera used to monitor the crack propagation.

Figure S20. ENF tests setup and specimen geometry used for this test. In the image on the right, the end of the initial crack a_0 = 55 mm is evidenced by the black line to help in observing the crack propagation, that results in a misalignment of the reference line.

The standard procedure followed in the lab is to monitor the crack propagation starting from the artificial crack (realized with a release film).

Every 5mm advance of the crack (observed in real-time from the DIC screen) a discharge-load cycle is carried out which will then be used if necessary to determine by correlation with finite element analysis the stiffness of the specimen.

The loading and unloading curves shall be performed at the following crack deflection values: 20 mm; 25 mm; 30 mm; 35 mm; 40mm; 50 mm; 55 mm; 60 mm; 65 mm. At the end of the test (after about 50 mm of propagation of the crack, then when it has reached 70 mm on the millimeter scale) the sample is discharged at a speed of 2mm/min and the test is concluded.

The data used for reprocessing are those extracted in .csv format from the DIC file, containing: transverse displacement (δ, obtained by marker); Force values and time. In particular the force-displacement curve is used for the next steps. By manual observation of the DIC images, the pairs of points deemed to be of interest are extracted from the curve and associated with the corresponding visually measured crack length (a). The choice of points of interest is made by avoiding the points following significant propagations of the crack and using, where possible, those immediately preceding them. This usually improves the quality of results. Starting from this data set, the four analytical procedures proposed by the legislation are followed:

1) Modified beam theory (MBT): $G_I=3P\delta/2ba$, where P = load; δ = displacement crosshead; b=gauge width; a=crack length.

2) Modified beam theory, corrected (MMBT): $G_I=3P\delta/(2b(a+|\Delta|))$, where Δ is a correction to the delamination length obtained by linear regression from graph C1/3-a, where C is the compliance obtained as δ/P.

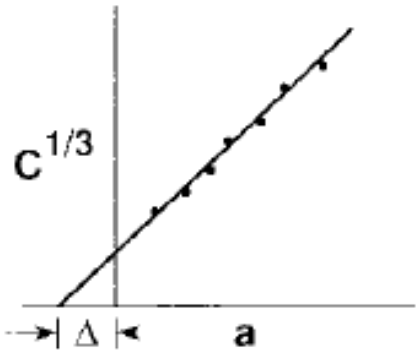

Figure S21: Graphical interpretation of the MMBT correction.

3) Compliance calibration (CC): $G_I=nP\delta/2ba$, where n is the slope of the log(C)-log(a) graph obtained by linear regression.

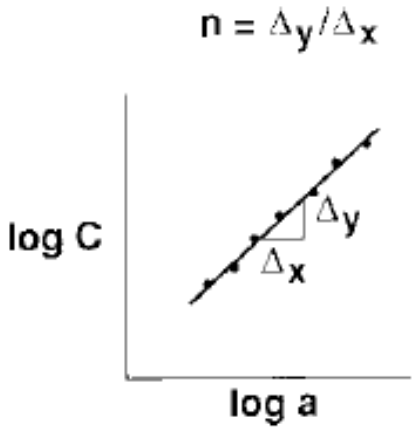

Figure S22: Graphical interpretation of the CC method.

4) Modified compliance calibration (MCC): $G_I=(3P\ 2\ C\ (2/3))/(2A1\ bh)$, where h=thickness of the test piece; A1=slope of curve a/h-C1/3.

For each test piece a curve called r-curve is then generated, with the displacement of the traverse δ on the X axis and the tenacity at fracture GI measured in N/mm on the ordinate's axis.

The calculation of the average value of GIC is carried out on the points of this curve, observing the following indications:

in cases where the curve shows a plateau area, only points belonging to that region are used;

where the plateau zone is not present, the mean is calculated on all points except the first (propagation from the crack apex with a form generated by the release agent due to the lack of pre-cracking phase).

During the procedure validation campaign, it was observed that the reprocessing method giving the most reliable results is the MMBT. The value taken as reference for GIC is therefore that obtained by this method.

Double Cantilever Beam (DCB) and End Notched Fracture (ENF) results

- DCB tests

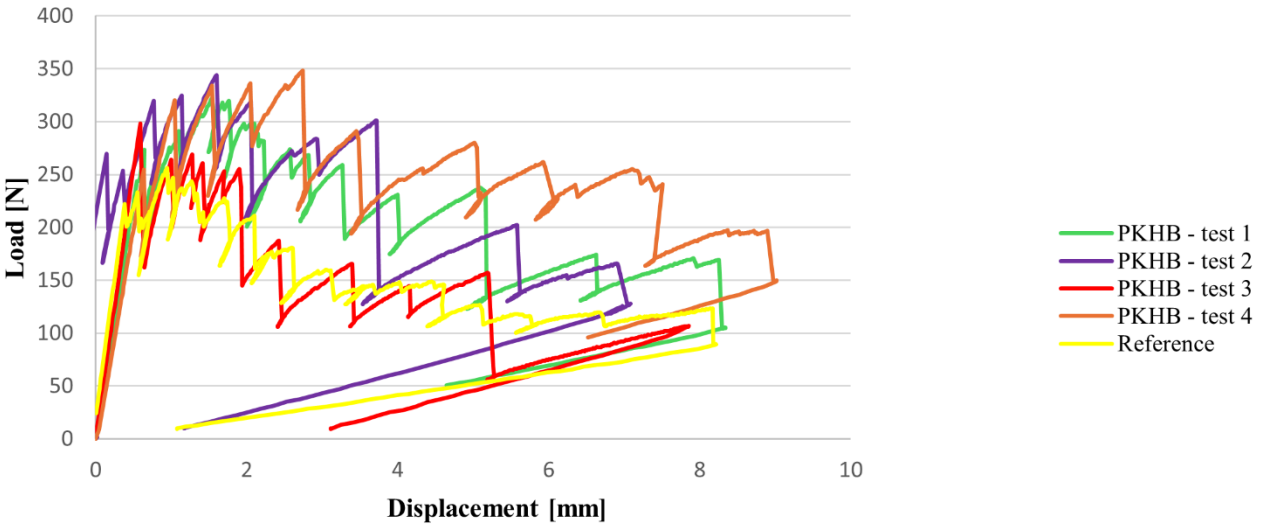

Figure S23. Load - displacement curves for PKHB specimens (colored lines) compared to average data of 4 reference specimens without any adhesive (yellow line).

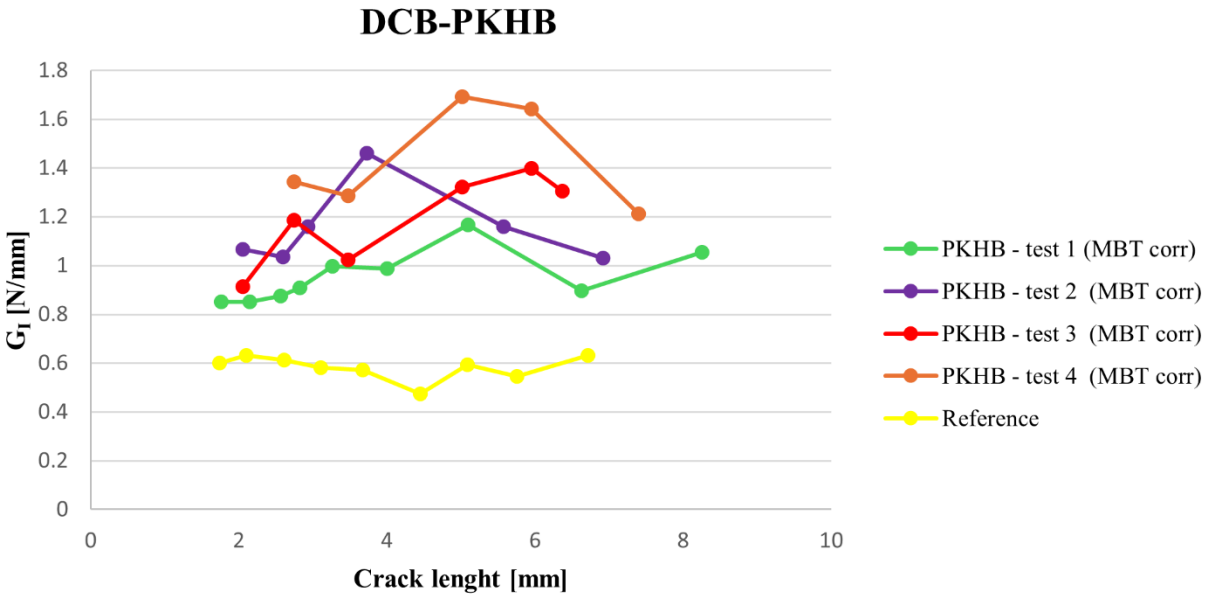

Figure S24. Resistance curves of PKHB adhesive compared to the reference.

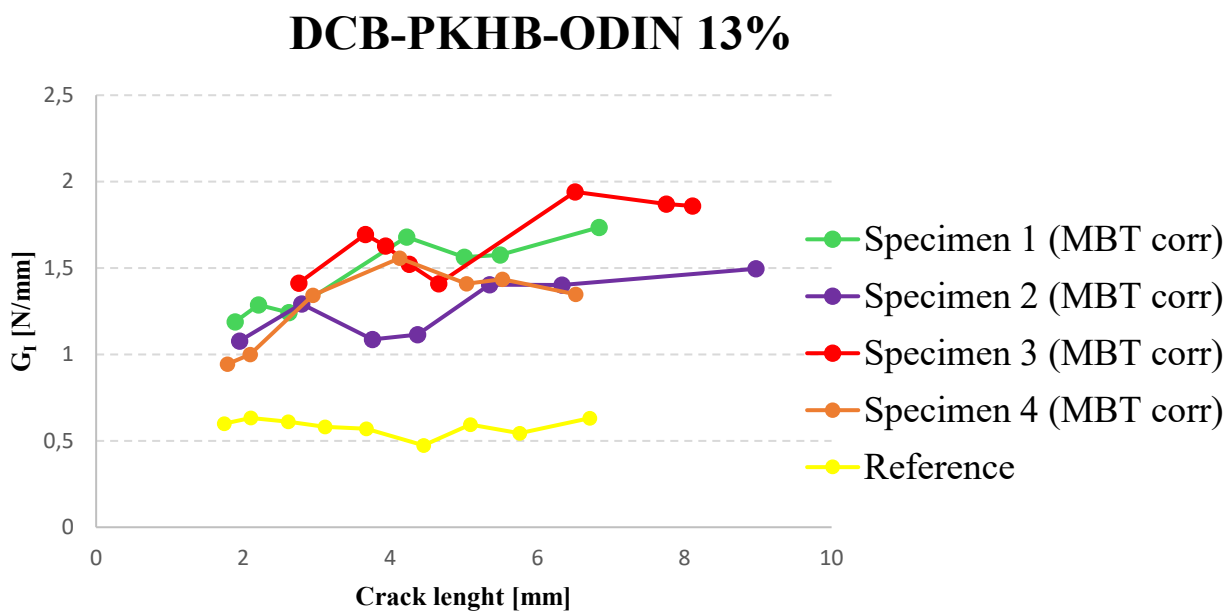

Figure S25. Resistance curves of PKHB-ODIN 13% adhesive compared to the reference.

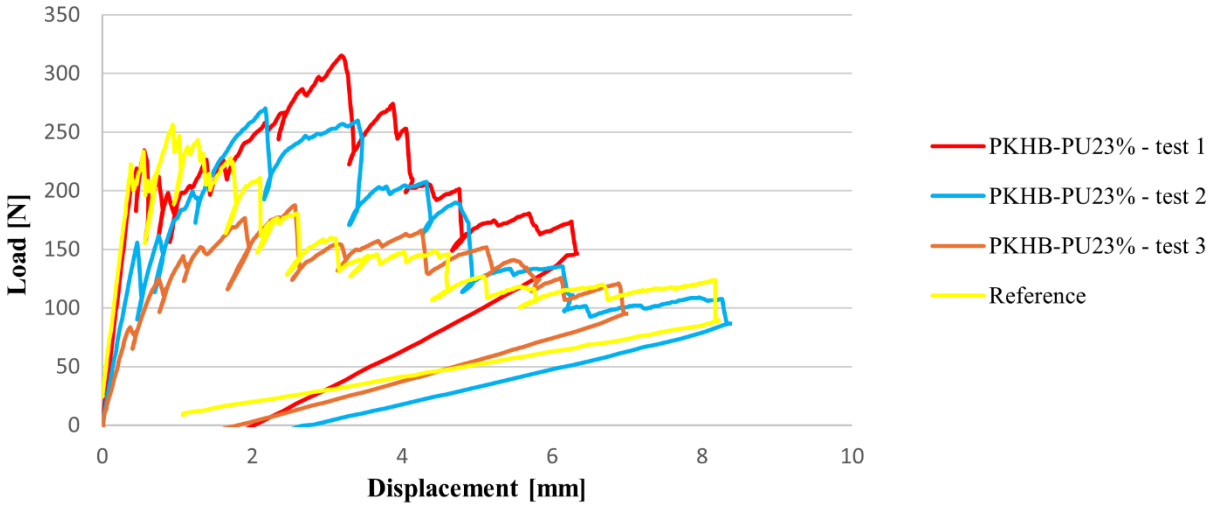

Figure S26. Load - displacement curves for PKHB-PU 23% specimens (colored lines) compared to average data of 4 reference specimens without any adhesive (yellow line).

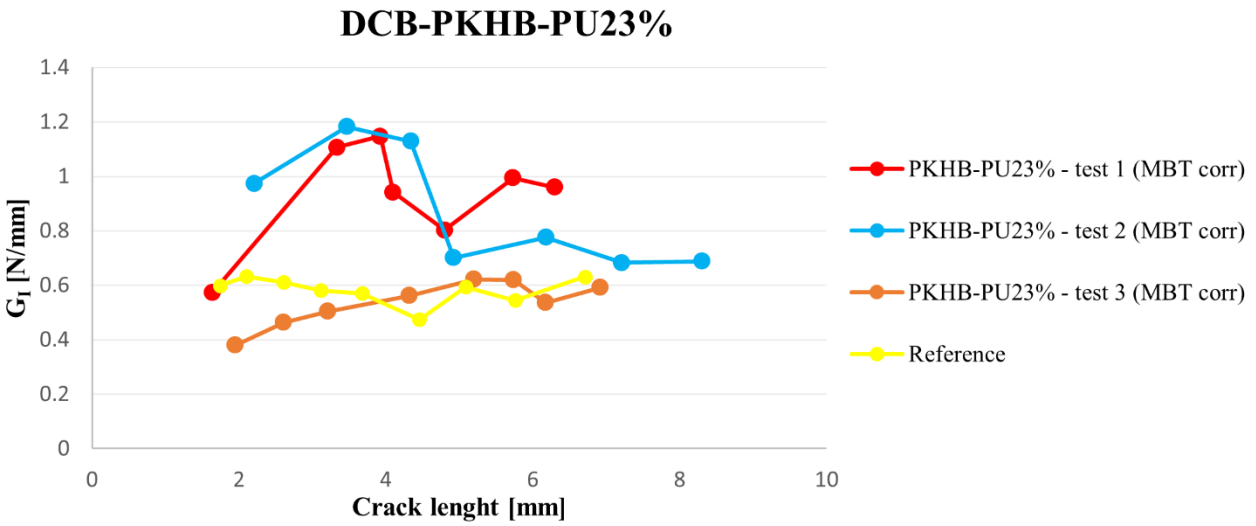

Figure S27. Resistance curves of PKHB-PU 23% adhesive compared to the reference.

Table S2: DCB test results for Reference specimens, PKHB, PKHB-ODIN 13% and PKHB-PU23% specimens. The values of G_I are calculated with the Modified Beam Theory Method. The fourth specimen measurement of PKHB-PU 23% was discharged due to the loss of the load point displacement by the DIC camera.

Reference	**Test 1**	**Test 2**	**Test 3**	**Test 4**	**Average [N/mm]**	**Standard Deviation [N/mm]**
G_I (MMBT) [N/mm]	0.551	0.582	0.603	0.617	0.588	0.029
PKHB	**Test 1**	**Test 2**	**Test 3**	**Test 4**	**Average [N/mm]**	**Standard Deviation [N/mm]**
G_I (MMBT) [N/mm]	0.954	1.152	1.191	1.435	1.183	0.197
PKHB-ODIN 13%	**Test 1**	**Test 2**	**Test 3**	**Test 4**	**Average [N/mm]**	**Standard Deviation [N/mm]**
G_I (MMBT) [N/mm]	1.467	1.267	1.667	1.291	1,423	0.185
PKHB-PU 23%	**Test 1**	**Test 2**	**Test 3**	**Test 4**	**Average [N/mm]**	**Standard Deviation [N/mm]**
G_I (MMBT) [N/mm]	0.932	0.876	0.557	/*	0,788	0.203

- ENF tests

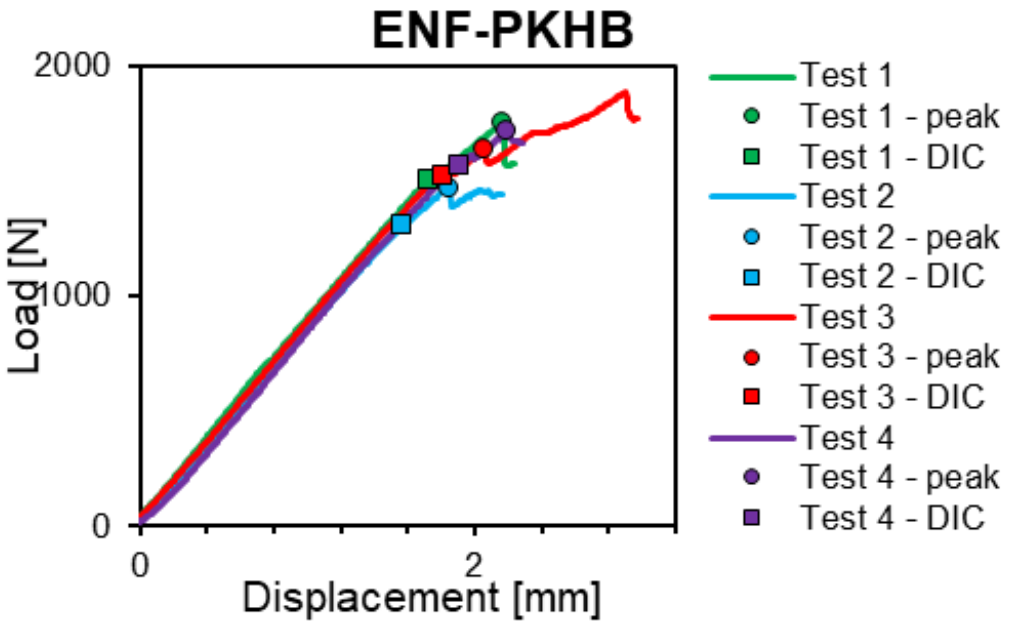

Figure S28. Resistance curves for PKHB specimens. The colored dots represent the point of crack propagation monitored by the MTS machine, while the colored circles represent the point of delamination determined by the DIC camera.

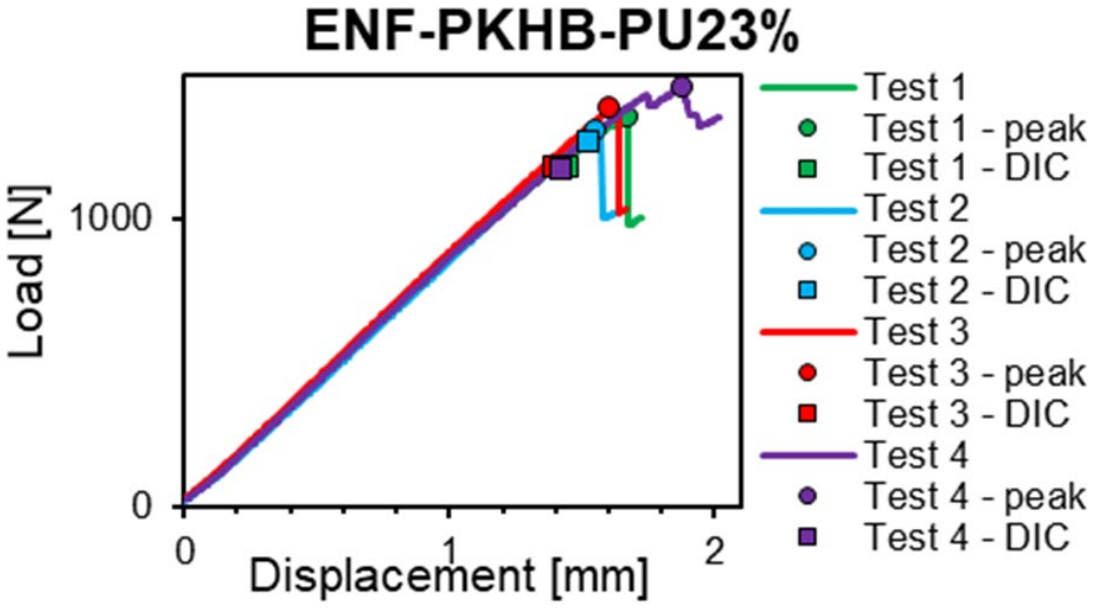

Figure S29. R-curves for PKHB-ODIN PU 23% specimen. The colored dots represent the point of crack propagation monitored by the MTS machine, while the colored circles represent the point of delamination determined by the DIC camera.

Table S3: ENF test results for Reference specimens, PKHB, PKHB-ODIN 13% and PKHB-PU 23% specimens. G_{II} (peak) refers to the G_{II} values calculated considering the load that corresponds to a drop in the load curve, while G_{II} (DIC) refers to the G_{II} values calculated considering the load corresponding to the first pixel dealignment of the adherends observed with the DIC camera.

Reference	**Test 1**	**Test 2**	**Test 3**	**Test 4**	**Average [N/mm]**	**Standard Deviation [N/mm]**
G_{II} (peak) [N/mm]	0.97	0.97	0.93	1.34	1,05	0.19
G_{II} (DIC) [N/mm]	0.96	0.96	0.94	1.34	1.05	0.19
PKHB	**Test 1**	**Test 2**	**Test 3**	**Test 4**	**Average [N/mm]**	**Standard Deviation [N/mm]**
G_{II} (peak) [N/mm]	1.72	1.38	1.70	2.02	1.70	0.20
G_{II} (DIC) [N/mm]	1.27	1.09	1.45	1.69	1.37	0.20
PKHB-ODIN 13%	**Test 1**	**Test 2**	**Test 3**	**Test 4**	**Average [N/mm]**	**Standard Deviation [N/mm]**
G_{II} (peak) [N/mm]	1.84	1.91	2.03	2.42	2.05	0.20
G_{II} (DIC) [N/mm]	1.54	1.37	1.54	1.48	1.48	0.02
PKHB-PU 23%	**Test 1**	**Test 2**	**Test 3**	**Test 4**	**Average [N/mm]**	**Standard Deviation [N/mm]**
G_{II} (peak) [N/mm]	1.13	1.00	1.14	1.27	1.13	0.04
G_{II} (DIC) [N/mm]	0.86	0.93	0.83	0.82	0.86	0.01

UV-Vis analysis

The absorption spectra of PKHB-ODIN 13% samples and PKHB-ODIN 13% dispersed (15% w/w) in epoxy-resin samples have an intrinsic contribution from the absorption of the polymeric matrix; the absorbance of the bare resin was measured and then subtracted from the sample after correcting for thickness variations, the results have been reported in Figure S31.

Absorption spectra of PKHB-ODIN 13% and PKHB-ODIN 13% dispersed (15% w/w) in epoxy-resin have been fitted with a linear combination of the absorption spectra of ODIN in DMSO (100% monomer) and ODIN in $CHCl_3$ (100% dimer). The results are reported in Figure S32: The dashed spectra in both panels represents the absorption spectra of ODIN molecule in pure monomeric form (dashed blue line) and in pure dimeric form (dashed gray line) respectively. Such conditions correspond respectively to the absorption spectrum of ODIN in DMSO and $CHCl_3$ solution. The red lines are the linear combination of monomer and dimer spectra that constitute the optimal fit to the experimental spectra. Linear combination allowed us to estimate that PKHB-ODIN 13% contains roughly the 35% of dimer form of ODIN, while for PKHB-ODIN 13% dispersed (15% w/w) in epoxy-resin the percentage of dimeric form is reduced to 15%.

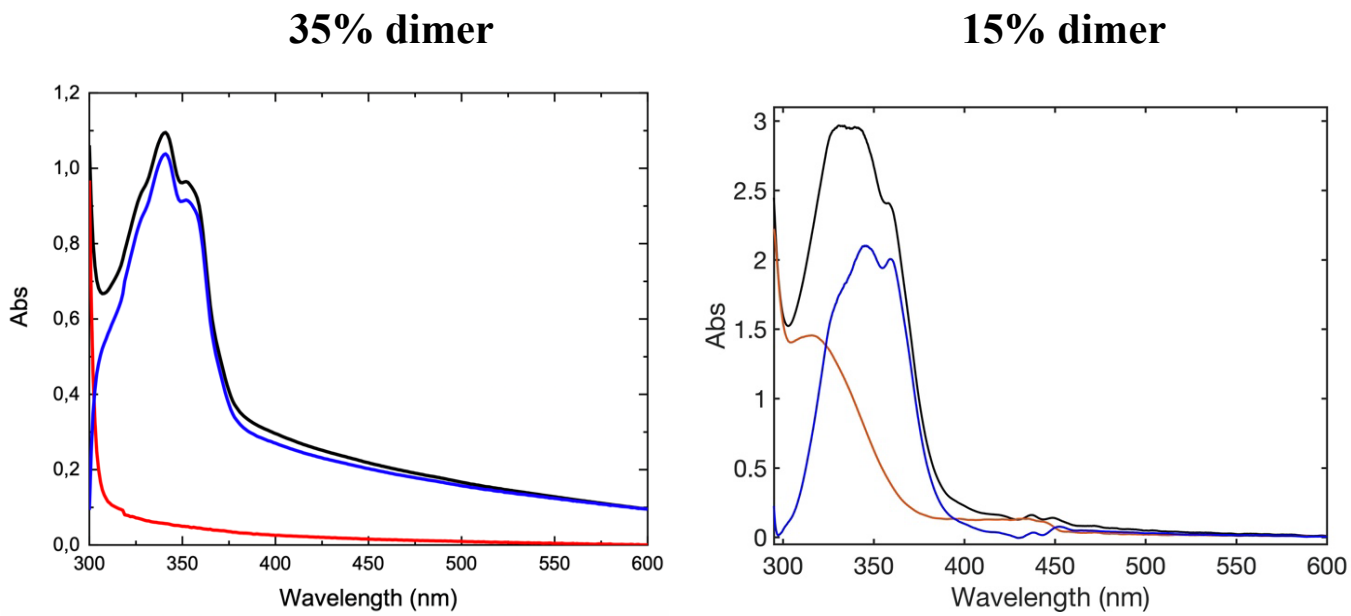

Figure S30. Absorption spectrum of PKHB-ODIN 13% (black line, left panel) and PKHB-ODIN-13% dispersed (15% w/w) in epoxy-resin (black line, right panel). The red lines are the absorption spectra of the resin substrates: PKHB (red line, left panel) and PKHB dispersed (15% w/w) in epoxy-resin. The blue lines are the corrected absorption spectra: a) PKHB-ODIN 13% corrected for the PKHB absorption (left panel); b) PKHB-ODIN 13% dispersed (15% w/w) in epoxy-resin corrected for the PKHB dispersed (15% w/w) in epoxy-resin absorption.

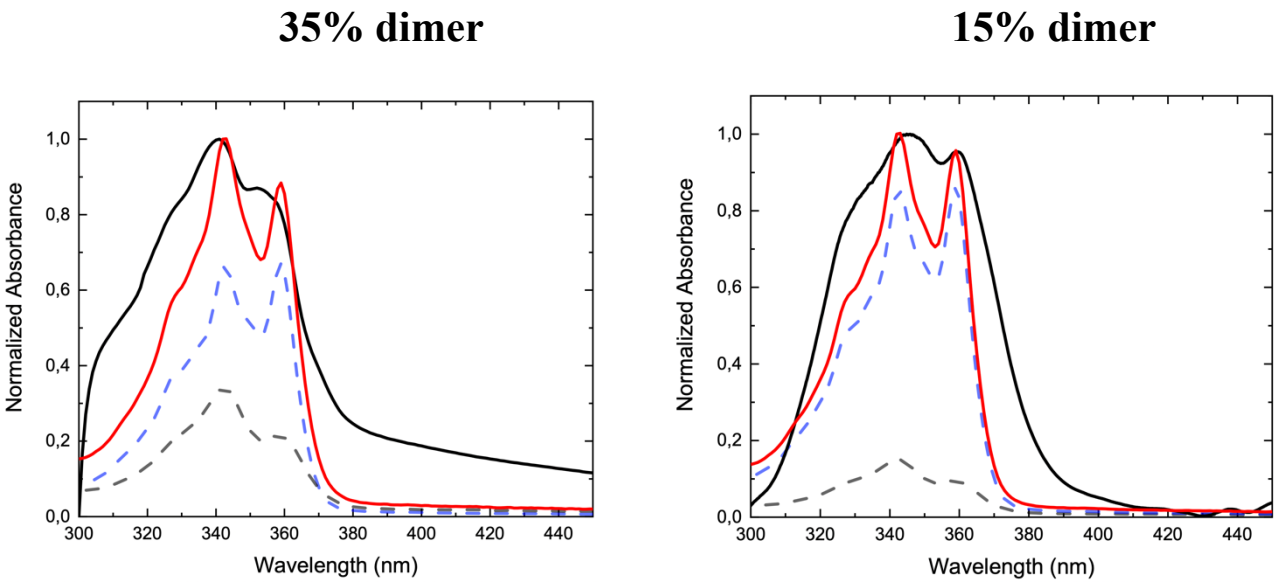

Figure S31. Experimental spectra of PKHB-ODIN 13% and PKHB-ODIN 13% dispersed (15% w/w) in epoxy-resin are reported as black lines respectively in left panel and right panel. The blue dashed spectra in both panels represents the absorption spectrum of ODIN in DMSO, while dashed gray line represents the spectrum in $CHCl_3$. The red lines are the linear combinations of blue and grey spectra that constitute the optimal fit to the experimental spectra (black lines).

SEM micrographs of DCB and ENF specimens

DCB (a)

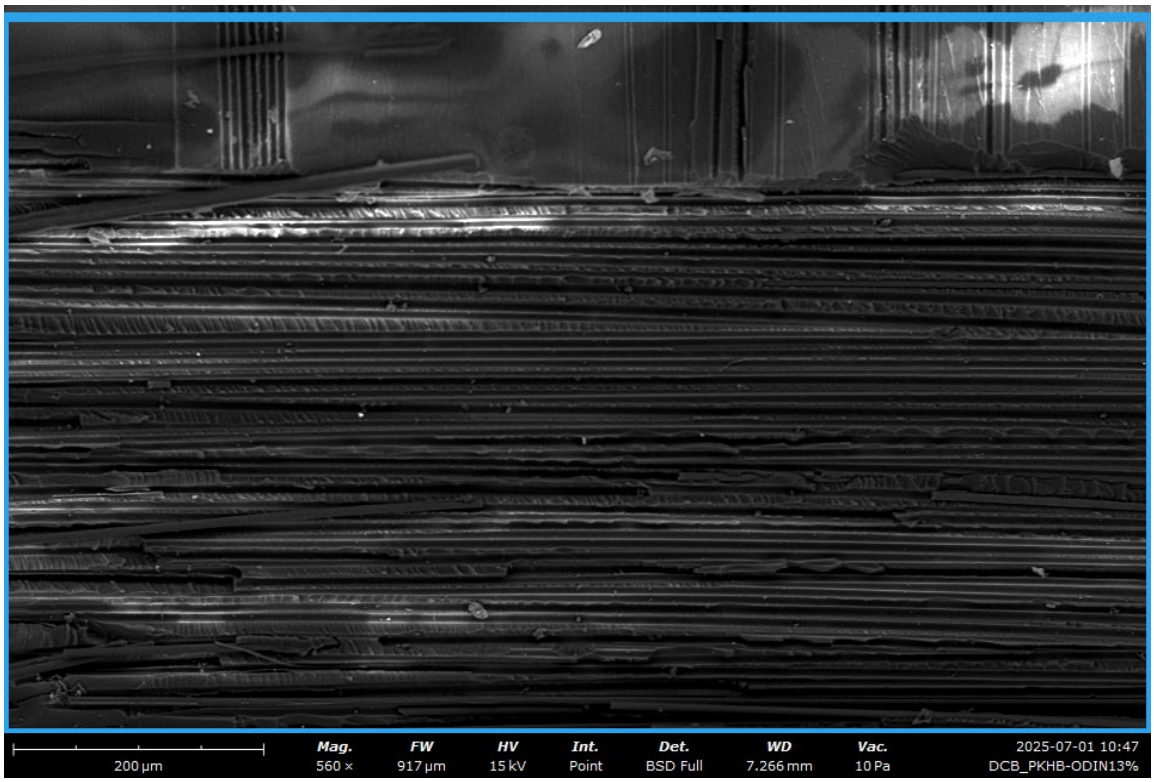

DCB (b)

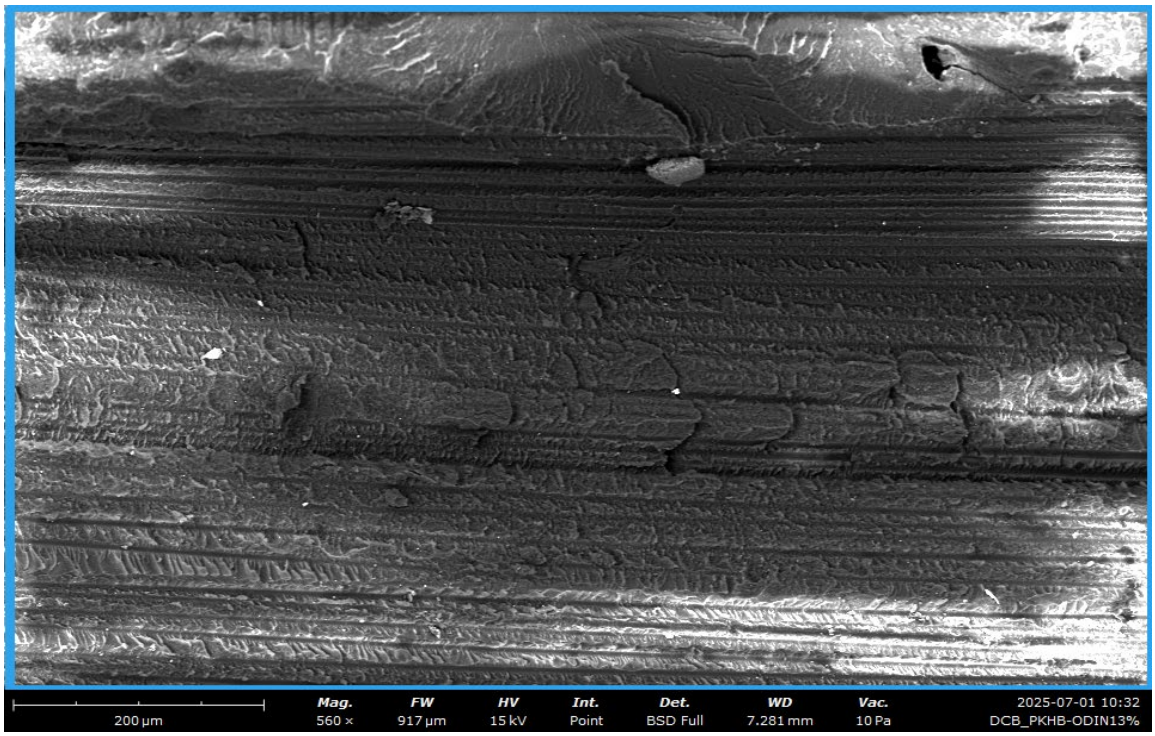

Figure S32. SEM micrographs of DCB failure surface of (a) reference specimen and (b) PKHB-ODIN 13% specimen.

ENF (a)

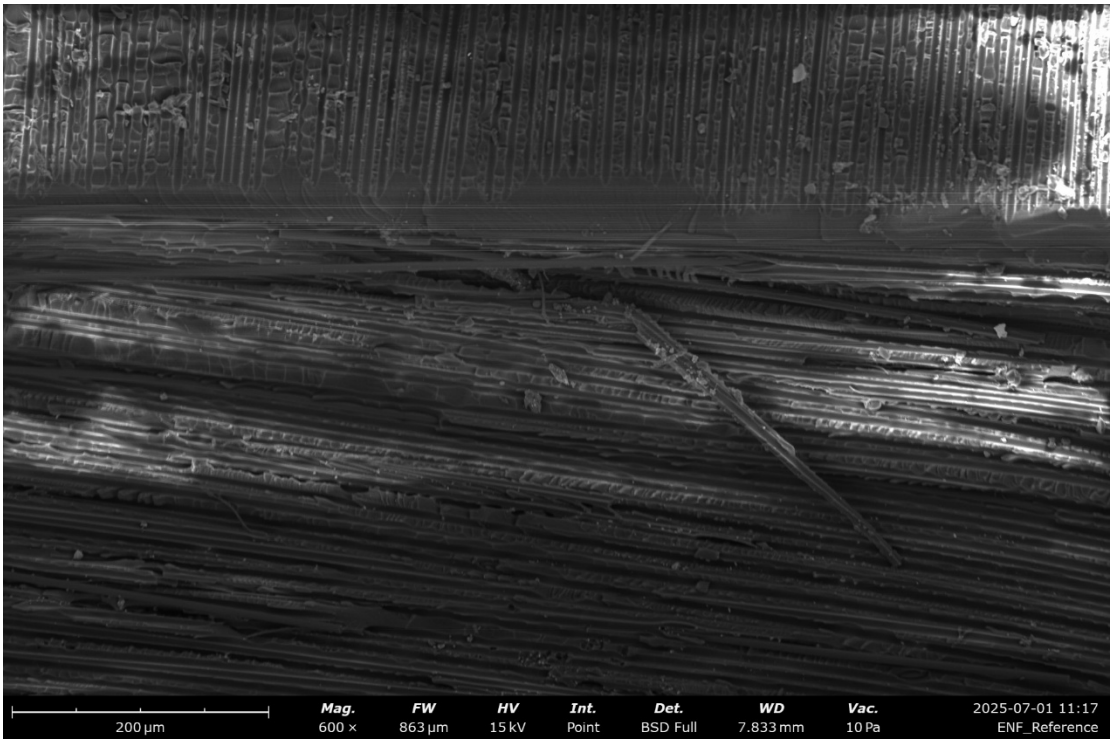

ENF (b)

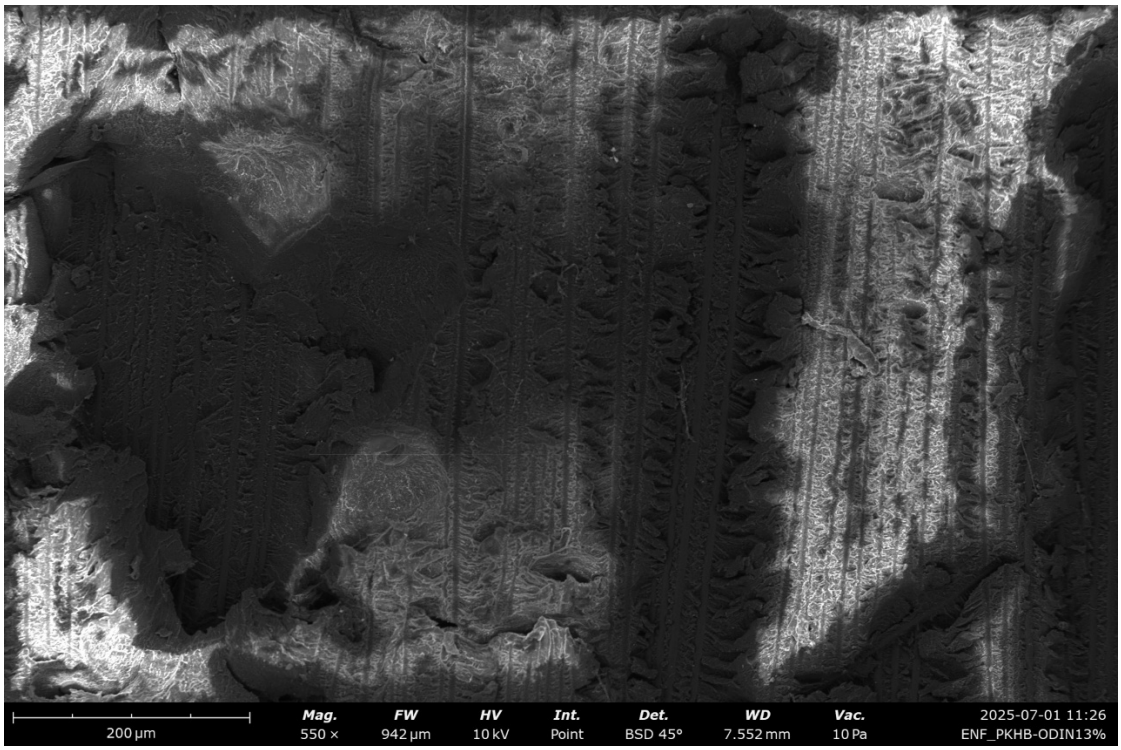

Figure S33. SEM micrographs of ENF failure surface of (a) reference specimen and (b) PKHB-ODIN 13% specimen.